Ger. Chem. Eng. 7 (1984) 72–84

Improvement of Clarification in Decanting Centrifuges*

Werner Stahl and Thomas Langeloh**

The theoretical design of decanting centrifuges has been based hitherto on the application of Stokes's law to the centrifugal field. This only takes account, in a general form, of the clarification surface of the decanter; other design data of the rotor, such as geometry of the screw conveyor or adjustment of the liquid height are not considered.

A better understanding of the effect of different machine settings on clarification in the decanter and a very good agreement with a simple theory is obtained on the assumption that, although suspended particles become settled according to Stokes's law, they do not remain on the bottom of the flow channel, formed by the screw, but are flushed to the overflow by the outflowing centrate.

1. Introduction and State of Knowledge from Theory and Practice

Decanting centrifuges are used in many branches of industry for a wide range of solid-liquid separation problems in processes in which the solids are heavier than the liquid. In addition to economical operation, compared to other methods employed in practice, these machines have a very stable operating behaviour; fluctuations in the feed with regard to particle density, solids concentration, viscosity etc. are "accepted" by the machine, and only the separation results vary monotonically. The possibility of operational failure, such as can occur on layer breakthrough in the pusher centrifuge, does not arise in the decanter.

Several workers have described the process engineering design, both in relation to the dewatering of solids [1, 2] and clarification of the centrate [3–6, 8–10]. Without discussing the individual publications in detail, it must be pointed out that the calculation methods, based on the theory of equivalent clarification area for predicting the solids content in the centrate, are inadequate, on their own, for a reliable scale-up for industrial application.

This applies in the first place to purely analytical procedures which attempt to predict the clarification result from physical properties of the product (viscosity, density difference and particle size distribution) in combination with the design data of the machine (diameter and clarification length, i.e. clarification area) and the operating parameters of the machine (rotational speed, differential speed, liquid height). Unfortunately, it is also largely true in the case of the more engineering-oriented approach, i.e. the transfer of actually measured separation results in a pilot decanter to an intended large scale machine, according to scale-up rules.

The only theory applied so far for the calculation of clarification is the Stokes's law, valid for the centrifugal force field; it describes, for the laminar regime, the sedimentation of a single rigid spherical particle in a quiescent Newtonian liquid.

This simplified model differs from real conditions in a decanter by virtue of the following effects which can be classified into two groups:

Product side:

- higher solids concentrations, as a result of interactions between particles,
- non-spherical particles,
- particle size distribution, no uniform particle size.

Machine side:

- no plug flow displacement of the liquid but unknown flow profile,
- flow disturbances due to outflow of the liquid in the screw conveyor channels,
- disturbances at the inlet and outlet of the clarification zone,
- effect of differential rotational speed of the screw and cross-section reduction by the sediment cake, etc.

Many workers have adapted Stokes's law to the measured values for the description of real processes occurring in the decanter, by introducing correction factors. With no intention of belittling these efforts, it must however be said that the current state of knowledge is unsatisfactory and the law cannot explain many phenomena.

This is seen most clearly when the effectiveness of the scale-up rule, based on this theory is examined. If the various correction factors are neglected (they must remain constant for similar types of decanters in larger versions) the relationship between the throughput, the still permissible particle size in the centrate and the machine data is as already given in [3]:

$$Q = \frac{4\pi^3}{9} \frac{\Delta\rho}{\eta} x_G^2 n_H^2 L_e \left(r_T - \frac{b_{Niv}}{2} \right)^2 . \qquad (1)$$

If the product data are kept constant and only the influence of geometry of a machine enlarged by the factor i is investi-

---

* Paper presented at the Annual Conference of Process Engineers in Basle on 1 October 1982.

** Prof. Dr.-Ing. W. Stahl and Dipl.-Ing. T. Langeloh, Institut für Mechanische Verfahrenstechnik und Mechanik der Universität Karlsruhe (TH), Kaiserstr. 12, D-7500 Karlsruhe.

 0343-5539/84/0203-0072$02.50/0

gated, the following results from formation of ratios:

$$\frac{Q_{main}}{Q_{model}} = \frac{n^2_{H,main}}{n^2_{H,model}} \frac{L_{e,main}}{L_{e,model}} \frac{\left(r_T - \frac{b_{Niv}}{2}\right)^2_{main}}{\left(r_T - \frac{b_{Niv}}{2}\right)^2_{model}}$$

$$= \frac{n^2_{H,main}}{n^2_{H,model}} ii^2. \qquad (2)$$

At identical centrifugal accelerations of the two machines, the following is valid for the main rotational speeds:

$$\frac{n^2_{H,main}}{n^2_{H,model}} = \frac{1}{i}, \quad \text{since} \quad (r\omega^2)_{model} = (r\omega^2)_{main}. \qquad (3)$$

In fact, at identical utilization of the capacities of the two rotors, not the acceleration but the rotor's circumferential velocity is kept constant. Since the circumferential stress in the rotor is proportional to the centrifugal speed, i.e. $u \propto rn$ = const, it follows that

$$\frac{n_{H,main}}{n_{H,model}} = \frac{1}{i}.$$

If the above throughput ratio is corrected accordingly, it follows that

$$\frac{Q_{main}}{Q_{model}} = \frac{i^3}{i} = i^2 \quad \text{or} \quad \frac{Q_{main}}{Q_{model}} = i, \qquad (4)$$

depending on whether the model test was performed on the assumption of identical centrifugal acceleration or identical circumferential velocity of the rotor.

This relationship is in contradiction to many results obtained in practice, whereby, at identical acceleration numbers, a capacity increase with the cube of the diameter was observed in similar machines.

Another result, obtained on applying Stokes's law to the solid bowl centrifuge, raises doubts: the liquid height does not affect the capacity of the machine; it can be deleted when applying this theory.

However, it is known from practice that the throughput rate exerts a strong influence on the liquid height. Because of this, nearly all the manufacturers design the cone with a small discharge diameter in order to allow the centrifuge to be run at high level setting.

Following this survey of the known approaches, the acknowledged discrepancies between more recent ideas will be discussed.

2. Experimental Investigations

A large number of experiments with decanters of widely varying sizes and with many different products have revealed the following clarification behaviour which is always observed, possibly with slight variations (Fig. 1).

When the machine parameters are kept constant, the solids content at first increases monotonically with the slurry throughput. The curve can start at the origin, but it can also begin at a low solids content. The limiting solids content at $Q \to 0$ cannot be measured; it is determined by back extrapolation. The measured values in this first range (1) show a slight scatter; after a delay period roughly equal to 10 times the liquid residence time, they become constant. The values are also readily reproducible when the throughput is either increased or reduced.

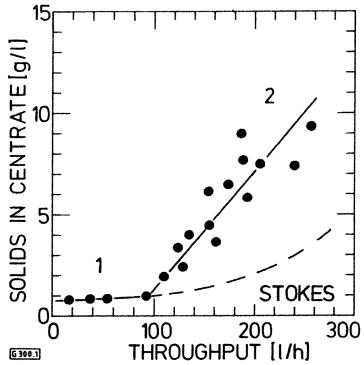

Fig. 1. Solids content in centrate as a function of throughput.

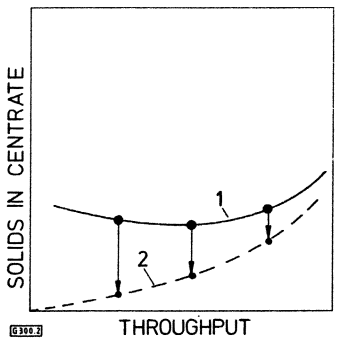

Fig. 2. Solids in centrate as a function of throughput. 1. Continuous operation. 2. Curve recorded point by point by disengaging the overload protection device.

At very small throughputs, the solids content in the centrate has, in many cases, been definitely linked to the differential speed of the screw conveyor. If the overload protection device of the machine is disengaged, i.e. the screw rotates at the same speed as the drum, a lower solids content is measured for a short time, subsequently gradually increasing as the rotor fills up with solids. An estimation of the disturbance effect of the screw motion can thus be obtained if the disengagement of the screw is applied at different throughputs (Fig. 2).

From a certain, highly reproducible throughput, referred to subsequently as Q_{crit}, the slope of the curve shown in Fig. 1 increases with increasing throughput, following a pronounced break. An increase of from one to two orders of magnitude is already being obtained at Q = 1.1 to 1.5 Q_{crit} (range 2). Moreover, it is evident that the values measured beyond the critical throughput show pronounced scatter which, however, cannot be dismissed as a measurement error because of the accuracy demonstrated at low throughputs. The measured values frequently lie between two diverging straight

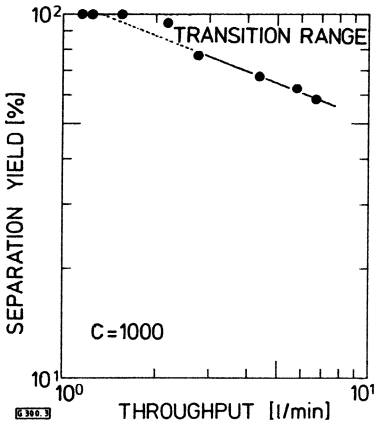

Fig. 3. Weakly defined break point; located by back extrapolation.

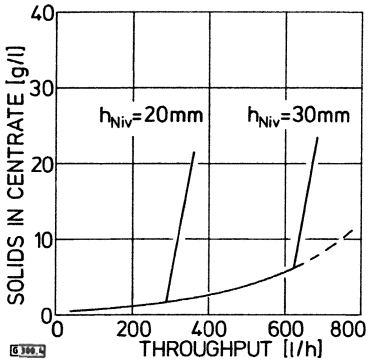

Fig. 4. Solids in centrate as a function of throughput for two different liquid heights (kaolin).

lines meeting at the point of the critical throughput (see Fig. 1). In some experiments it was shown that a hysteresis behaviour appears to prevail close to the critical throughput; at very slowly increasing throughputs, good clarification results are sometimes still obtained beyond the Q_{crit} point which can, therefore, often be determined more precisely by back extrapolation than by direct measurement (Fig. 3).

This solids content profile cannot be explained in terms of the limiting grain size calculated by Stokes's law for different throughputs (Figs 16a and b).

The observed effect is particularly undesirable in industrial practice, since established limiting values (guaranteed values) of the solids content are immediately exceeded several times.

In addition to the unanswered question of the physical cause of this behaviour, it is first attempted to solve experimentally the following problems: How does the position of the break depend on the freely changeable variables, i.e. level height, absolute and differential speed of the decanter?

It was shown possible to shift the break point into the range of higher throughputs by increasing the liquid height, whereby the already known steep second branch starts at the base curve which increases monotonically with the throughput (Fig. 4).

It has been found both, from own experiments [14, 15] and

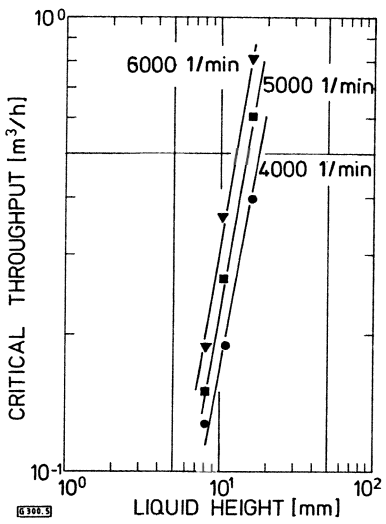

Fig. 5. Critical throughput as a function of liquid height (D-beads, [11]).

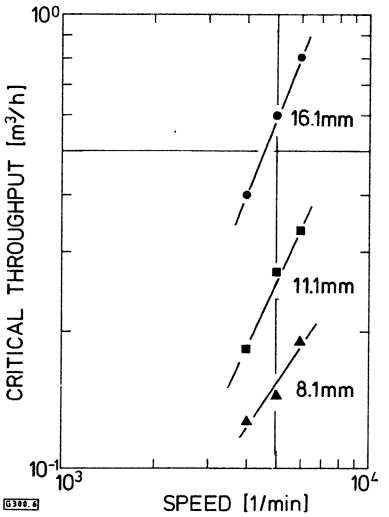

Fig. 6. Critical throughput as a function of absolute rotational speed (D-beads, [11]).

from an evaluation of the results in [11–13] that the throughput Q is roughly proportional to h^2_{Niv} (Fig. 5).

The effect of the main rotational speed produced experimentally less precise results. The exponent however was of the order of 2 or less (Fig. 6).

A relationship between the critical throughput and differential speed was only observed when the latter was set too low, which resulted in a build-up of solids in the clarification part, or was set extremely high, which is never advisable for clarification purposes.

As can be seen from Fig. 3, the differential speed which varied in the range 1 : 3 does not affect the separation efficiency.

Anton [12] has also established, as shown in Fig. 7, that the differential speed cannot change the positions of the break points of the efficiency curves.

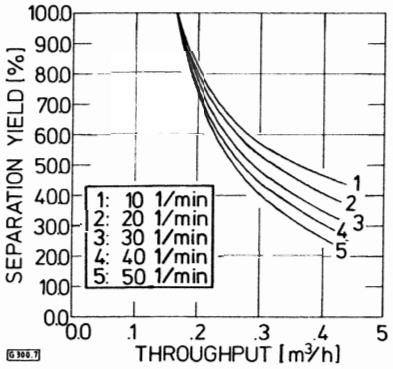

Fig. 7. Effect of differential speed on clarification [12].

Instead of solids content in the centrate, the expression of separation efficiency (difference between solids flow in feed and that in the centrate based on the solids flow in feed) is plotted which, in process engineering, is also frequently referred to as solids yield. Tests with variations in the screw geometry have not yet been performed by the authors for reasons of time and cost. Nevertheless, on the basis of own results described above, an evaluation of literature and other experience which cannot be detailed here, a concept of the physical process underlying this non-steady behaviour has been developed.

3. The Drag Effect

The presence of random fluctuations in the clarification behaviour of countercurrent decanters and its quantitative relationship leads to the conclusion that an additional effect is superimposed on the normal monotonically deteriorating precipitation behaviour, which can be determined approximately at least in zones of very small solids concentrations with the aid of Stokes's law using the correction factors described in literature [8–10]. This effect, if it occurs beyond Q_{crit}, does fully control the chain of events. This second relation then supersedes the modified Stokes's law in the sense of a yes-no decision.

The following representation can be formulated:

The shear stress in the liquid at the surface of the deposited solids layer, which increases with increasing throughput, causes the already settled solid particles to migrate. They are entrained with the liquid in a spiral direction, through the flow channel formed by the conveyor blades, and discharged over the weir at the end of the rotor.

This sliding or rolling of the particles on the surface of the solids base layer in the drum is a process which depends both on the particle shape and size, liquid viscosity, obviously on the flow profile, but also on such imponderables as the state of wear of the screw and the associated profile of the grooves cut into the base layer.

A similar process of entrainment of deposited particles occurs in nature in every river bed. The drag effect disappears and stabilized sedimentation occurs when the flow velocity of the river decreases; this can be observed at estuaries and leads to the known phenomenon of delta formation.

4. Formulation of the Drag Effect

Although this process in the decanter, at operating conditions involving a substantial solids content in the centrate, can certainly be represented as entrainment of particle swarms in a strand formation, in which mutual interaction between the particles does also occur, it still appears justified to apply some simplifications to the initial mathematical formulation of this process. Let us assume that a single spherical particle rests, in a laminar flow regime, on the inner surface of a drum covered by a base product layer and is exposed to the centrate flow in the screw channel. Since the primary aim of the following discussion is not to assess the separation efficiency in the range $Q > Q_{crit}$, but rather to localize the limiting case Q_{crit}, the simplified assumption that just a few particles are flushed out near the discharge end of the decanter is well justified.

Fig. 8 shows the force relationships at this particle. It is pressed onto the base with compression force F_A:

$$F_A = \frac{\pi}{6} x^3 \Delta\rho g C. \tag{5}$$

Let a frictional force F_H prevail between the particles and the base, opposite to the sliding or rolling motion which, for the sake of simplicity, is assumed to be proportional to the compression force, in accordance with Coulomb's friction law:

$$F_H = f F_A. \tag{6}$$

The following applies to the drag force on a stationary spherical particle in a shear flow:

$$F_s = \underbrace{\frac{\pi}{4} x^2}_{\text{cross-sectional area of the particle}} \times \underbrace{\eta}_{\text{viscosity of the liquid}} \times \underbrace{\kappa}_{\text{shear gradient}} . \tag{7}$$

A relationship between the centrate throughput of the decanter and the shear gradient at the base is obtained on the assumption of a laminar planar layer flow (parabolic profile):

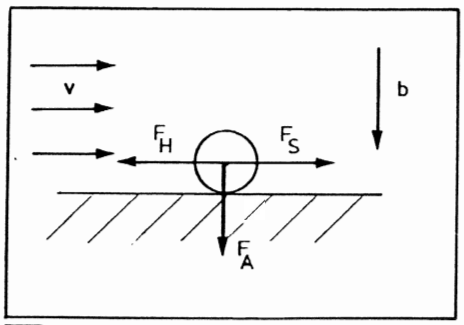

Fig. 8. Balance of forces around a particle already separated (drag force formulation).

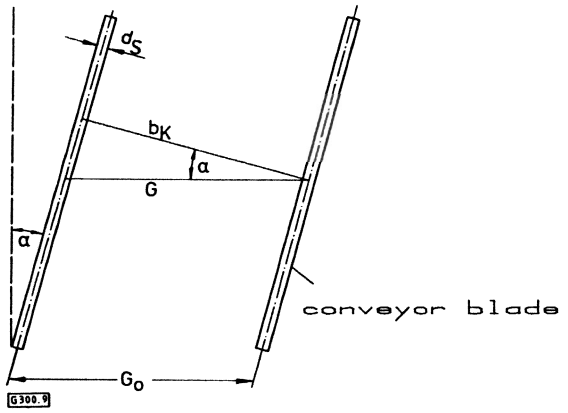

Fig. 9. Relationship between channel width and the helical conveyor geometry.

$$\kappa = \left(\frac{du}{dz}\right)_{z=0} = \frac{3v_m}{b_{Niv}} = \frac{3Q}{b_{Niv}b_{Niv}b_K}. \tag{8}$$

It is clear from the sketch (Fig. 9) that the channel width resulting from the screw data is:

$$b_K = G\cos\alpha - z_s d_s \tag{9}$$

and hence

$$\kappa = \frac{3Q}{b_{Niv}^2(G\cos\alpha - z_s d_s)}. \tag{10}$$

If this expression is substituted in the above equilibrium of forces for the horizontal direction, it follows that:

$$F_H = F_S,$$

$$f\frac{\pi}{6}x^3\Delta\rho gC = \frac{\pi}{4}x^2\eta\frac{3Q}{b_{Niv}^2(G\cos\alpha - z_s d_s)}, \tag{11}$$

$$Q = f\frac{2}{9}gC\frac{\Delta\rho}{\eta}xb_{Niv}^2(G\cos\alpha - z_s d_s). \tag{12}$$

This equation can now also be solved with respect to particle size, which yields the drag particle size:

$$x_s = \frac{9Q\eta}{2fgC\Delta\rho b_{Niv}^2(G\cos\alpha - z_s d_s)}. \tag{13}$$

This particle size determines, as does the limiting particle diameter according to Stokes's law for sedimentation, which particles still just adhere to the base layer and which ones are flushed out with the centrate.

The friction coefficient is calculated from:

$$f = \frac{9Q\eta}{x_s 2gCb_{Niv}^2(G\cos\alpha - z_s d_s)\Delta\rho}. \tag{14}$$

Comparison of the two laws illustrates the analogy:

$$Q = \text{const}\ \frac{\Delta\rho}{\eta}x_G^2\ Cg\ L_e\left(r_T - \frac{b_{Niv}}{2}\right), \quad \text{(Stokes)}$$

$$Q = \text{const}\ f\frac{\Delta\rho}{\eta}x_s\ Cg\ b_{Niv}^2(G\cos\alpha - z_s d_s), \quad \text{(drag force)}$$

$$x_G = \text{const}\ \sqrt{\frac{\eta}{\Delta\rho}}\ \sqrt{\frac{Q}{Cg}}\ \sqrt{\frac{1}{L_e(r_T - b_{Niv}/2)}}, \quad \text{(Stokes)}$$

$$x_s = \text{const}\ \underbrace{\frac{1}{f}\frac{\eta}{\Delta\rho}}_{\text{physical data}}\ \underbrace{\frac{Q}{Cg}}_{\text{operating data}}\ \underbrace{\frac{1}{b_{Niv}^2(G\cos\alpha - z_s d_s)}}_{\text{machine data}}. \quad \text{(drag force)}$$

Therefore, it must be accepted that there exist two mutually independent limiting particle sizes, whereby the larger one always limits the throughput.

Obviously, the friction coefficient f cannot be obtained directly by measurement; it must, if necessary, be determined in a decanter experiment. In connection with the particle size distribution of the feed slurry, the following operational states are possible:

If $x_{min} < x_s < x_G$ or $x_{min} < x_G < x_s$, the separation efficiency is, in principle, already less than 100% (Fig. 10). At the critical throughput, the limiting particle size is identical to the drag particle size, i.e. both laws apply simultaneously. For throughputs smaller than Q_{crit}, Stokes's law applies and, for higher throughputs, the drag force equation describes the separation.

For determination of f, the particle size can be calculated from Stokes's equation and substituted into Eq. (14). This however assumes that, without corrections, Stokes's law yields the correct particle size.

The second, practically more important case, exists when $x_G < x_s < x_{min}$ and $x_s < x_G < x_{min}$ (Fig. 11). At first, complete separation occurs until, at a further increase in throughput, x_s or x_G become respectively equal to x_{min}.

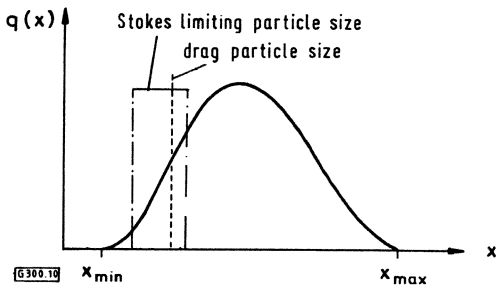

Fig. 10. Particle size distribution: $x_{min} < x_s < x_G$ and $x_{min} < x_G < x_s$.

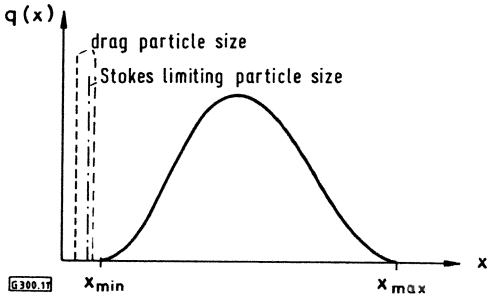

Fig. 11. Particle size distribution: $x_s < x_G < x_{min}$ and $x_G < x_s < x_{min}$.

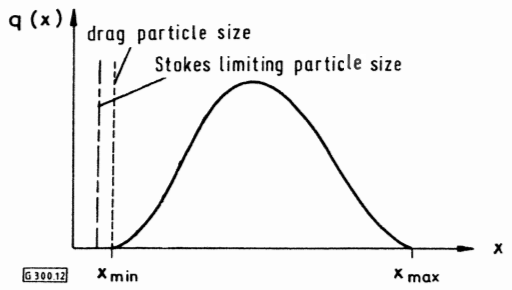

Fig. 12. Particle size distribution: $x_s = x_{min} > x_G$.

When $x_s = x_{min} > x_G$, in order to calculate the friction coefficient f, the critical throughput Q_{crit} is substituted for Q in Eq. (14) and the smallest particle diameter of the solid x_{min} for x_s (Fig. 12). In this case the separation is described only by the drag force relationship.

The overlapping of the two laws is the result of different throughput effects on the limiting particle diameter ($x_G \propto \sqrt{Q}$) and drag diameter ($x_s \propto Q$).

This knowledge permits a consideration of five important topics, i.e.:

- comparison of theory with measured results,
- attempt to predict separation efficiency for the range $Q > Q_{crit}$,
- scale-up methods taking into account the drag effect,
- operating consequences for the use of decanters in industry,
- constructional consequences for the design of new and improvement of existing decanters.

5. Comparison of Theory with Measured Results

If the primary aim is the interconversion of operational settings of a single decanter, this theory can be verified by forming a dimensionless parameter:

$$\frac{Q}{n_H^2 b_{Niv}^2}.$$

This is shown again in Fig. 13a for the already mentioned results of [11].

Considering that, with the altered main rotational speed, the differential rotational speed has also changed in the ratio 1 : 1.5 due to the constant gear ratio and, on account of level change in the range 1 : 2, the flow profile is slightly altered at the same time (adhesion conditions not only at the bottom but also on the screw flanks), the existing deviations must still be regarded as very small.

Analogous plotting, according to the theory of equivalent clarification area, as shown in Fig. 13b, would not produce agreement.

A different result is obtained in an industrial machine, over 600 mm in diameter, used for a flocculated slurry of a very fine mineral sludge. A plot against an extended characteristic parameter, at given variations of the C-value, liquid height and liquid viscosity, varying here for operational reasons, shows very useful results for the conditions of a field test carried out during production (Fig. 14).

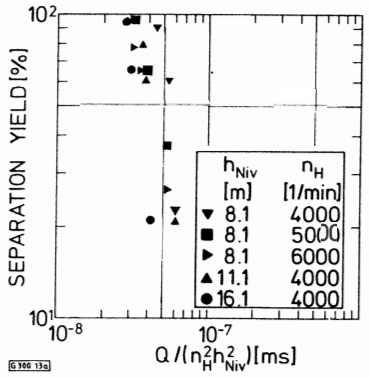

Fig. 13a. Representation of experimental results obtained by Kannenberg against the parameter $Q/(h_{Niv}^2 n_H^2)$.

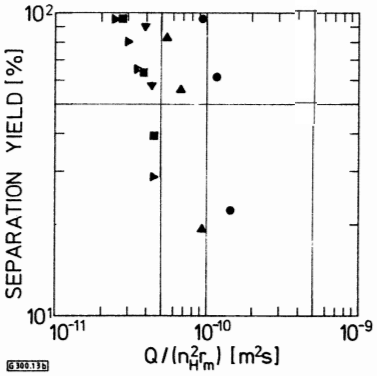

Fig. 13b. Representation of experimental results obtained by Kannenberg against the parameter $Q/(n_H^2 r_m)$; measuring points see Fig. 13a.

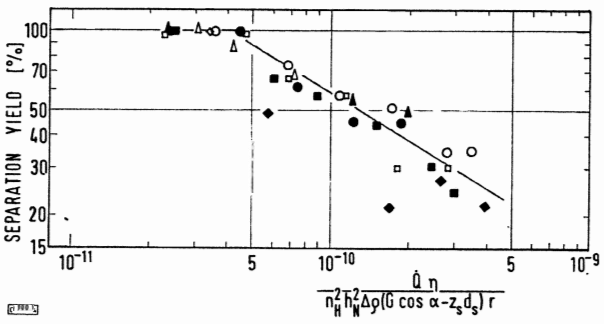

Fig. 14. Separation efficiency for a mineral slurry.

		large machine				small machine	
		□	○	●	■	◆	▲
C-value	[–]	1000	1000	1000	700	500	1000
differential speed of conveyor screw	[1/min]	20	15	15	20	20	20.8
liquid height	[mm]	90	65	100	90	90	30

It should be noted that this diagram also shows the previously conducted pilot tests with a small decanter.

Although the relationship between the shear gradient and the centrate throughput was only derived for the laminar case, the quadratic dependence on the liquid height has also been shown at channel Reynolds numbers in excess of 15,000. The liquid height was varied from $h_{Niv} = 0.08$ to $0.31\, r_T$.

The influence of the flow profile in the screw channel requires verification during the intended research work. It is to be expected that, with increasing Reynolds number the exponent will become less than two (influence of turbulence).

As a provisional finding, it can be concluded that, for assessment of different machine settings of a decanter, the break point in the separation efficiency curve, given by

$$K_s = \frac{Q_{crit}\eta}{n_H^2 b_{Niv}^2 (G\cos\alpha - z_s d_s)\Delta\rho r}$$

is appropriate.

6. Attempted Prediction of Separation Curve for the Range $Q > Q_{crit}$

Although a recovery of less than 100% can only be tolerated in a small number of applications and, therefore the curve shape is much less important for the practical engineer than the knowledge of the position of the break point, it should nevertheless be briefly discussed.

With increasing throughput, x_s in the particle size distribution is displaced towards larger diameters and, depending on the shape of the distribution curve (see Fig. 15), a faster or slower increase in the solids content of the centrate is observed. In the limiting case of a uniformly sized slurry in the feed, it would be expected that, on intersection of x_s and x_{prod}, clarification would break down suddenly, i.e. the separation efficiency falls vertically from the critical throughput.

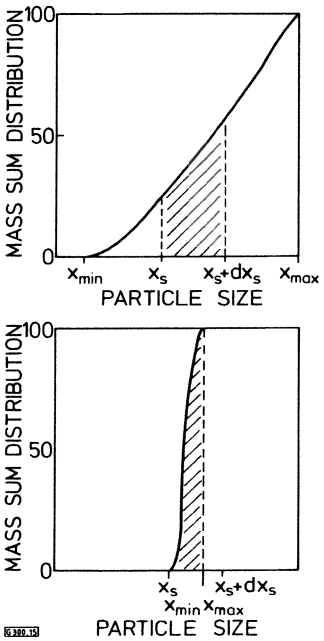

Fig. 15. Effects of displacement of the entrained particle diameter at different particle distributions.

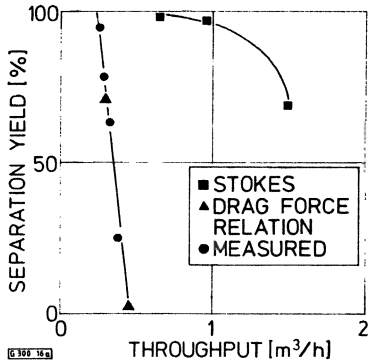

Fig. 16a. Separation yield as a function of throughput at $n_H = 6000$ 1/min, $b_{Niv} = 8.1$ mm.

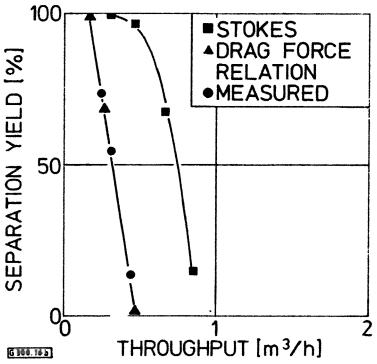

Fig. 16b. Separation yield as a function of throughput at $n_H = 4000$ 1/min, $b_{Niv} = 11.1$ mm.

Obviously, this classification behaviour is not so pronounced in industrial suspensions; particularly at higher solids concentrations, fine material will sink together with the coarser grains and become incorporated in the sedimented cake.

This method of calculation can still be used as an approximation, as shown by the results of Fig. 16, which originate from measurements by Kannenberg [11].

As early as 1962, he found that the measured separation curves neither agreed with those predicted by Stokes's theory nor showed similar behaviour.

If the results are calculated according to the drag force law, setting $x_{min} = x_s$ for the break point for the narrow fraction used, the calculated values describe the profile very precisely (Fig. 16).

7. Scale-up Methods Incorporating the Drag Effect

Since drag coefficients for different products and machine conditions are largely unknown, it is essential to determine the break point in a pilot trial and to transfer its position

to machines of other sizes, geometries and operational settings. This also has the advantage that the drag effect, occurring under machine conditions, is measured globally and assumptions or imprecise laboratory measurements of coefficient f and the possible associated transfer errors can be neglected.

The above derived relation for the critical throughput can be expressed as follows, combining the product data which naturally remain unchanged on scale-up:

$$Q_{crit} = \text{const} \underbrace{C T}_{S} \qquad (15)$$

S = equivalent traction coefficient,

where

$$C = \frac{r\omega^2}{g},$$

$T = b^2_{Niv}(G \cos\alpha - z_s d_s)$ = traction coefficient; it summarizes all constructional values.

The product of the two will be referred to as the equivalent traction value.

If a slurry is processed in two decanting centrifuges of different sizes and at identical accelerations, in the machine larger by the enlargement factor i, the following displacement of the critical throughput occurs:

$$\frac{Q_{crit,main}}{Q_{crit,model}} = \frac{\text{const } T_{main}}{\text{const } T_{model}} = \frac{b^2_{Niv}(G \cos\alpha - z_s d_s)_{main}}{b^2_{Niv}(G \cos\alpha - z_s d_s)_{model}}, \qquad (16)$$

and, since all values of the main version are larger by i,

$$\frac{Q_{crit,main}}{Q_{crit,model}} = \frac{b^2_{Niv,model} i^2}{b^2_{Niv,model}} \times \frac{(G \cos\alpha - z_s d_s)_{model} i}{(G \cos\alpha - z_s d_s)_{model}} = i^2 i = i^3. \qquad (17)$$

This cubic relationship has frequently been confirmed by measurement but the liquid volume of the drum was regarded as a reference value for the throughput rate, without a known physical reason. With geometrically dissimilar machines, a separate evaluation can now be made according to the influence of the liquid height and the screw pitch.

Incidentally, the drag law shows a complete analogy to the theory of the equivalent clarification area Σ, first described by Smith, Hebb, Ambler and Trawinski, according to which the critical throughput of the decanter is larger than that of a clarification tank by the factor C of effective accelerations. The tank is in the gravitational field, and has an identical clarification surface area A:

$$Q_{crit} = \underbrace{w_{st} C A}_{\Sigma} \qquad (18)$$

Σ = equivalent clarification area.

In addition to these, already mentioned and hitherto exclusively used parameters A and Σ, analogous and independent coefficients T and S will have to be used, to incorporate capacity limitation due to the drag effect on the particles.

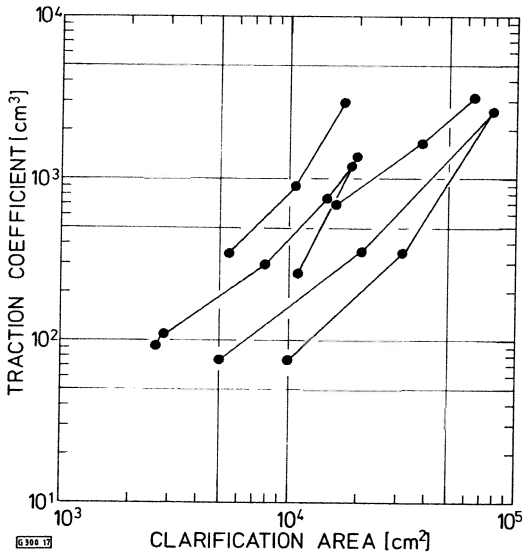

Fig. 17. Traction coefficient as a function of clarification area for various decanters.

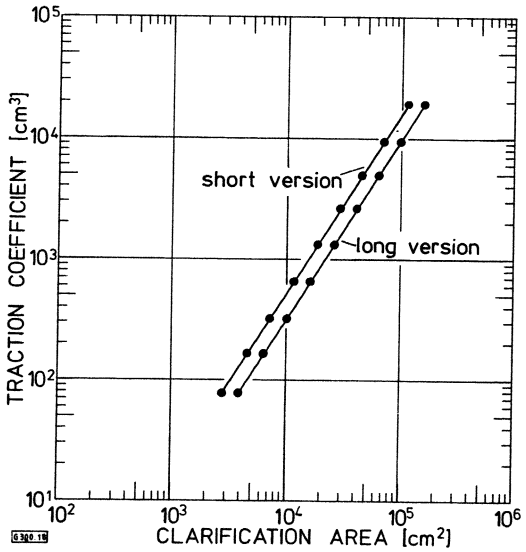

Fig. 18. Traction coefficient as a function of clarification area for the assumed decanter series.

The larger the value T of a decanter, the more can the throughput increase without occurrence of a drag effect.

Fig. 17 shows the data of several decanters made by different manufacturers and of different sizes. In the absence of precise data, the maximum level height was set for all the machines in such a way that between the maximum liquid height and the solids discharge radius there exists a difference amounting to 10% of the cylindrical drum radius. Machines of different sizes, made by the same manufacturer, are connected by straight lines.

For machines of different sizes and absolutely similar geometry, as e.g. calculated in Fig. 18 with two hypothetical

types of series R10, i.e. with an enlargement factor of consecutive sizes of $i = 1.25$, a straight line with a slope of 1.5 is obtained in a log-log representation, since the ordinate increases with the cube and the abscissa with the square of the enlargement factor.

Table 1 lists, for two hypothetical construction series, differing from one another only by the clarification length, the traction coefficient, the equivalent traction coefficient, the clarification area and the equivalent clarification area.

The following realistic assumptions have been made:

$b_{Niv,max} = 0.15\ d_T$,
$G = 0.25\ d_T$,
$d_s = 0.015\ d_T$,
$L_{cyl} = 1.5$ and $2.0\ d_T$.

On account of the geometrical similarity, the screw pitch angle ($\tan \alpha = G/(2\pi r_T) = 0.0796$) with $\alpha = 4.55°$ is constant for all sizes; $\cos \alpha$ is therefore approximately unity.

The same real machines are plotted in Fig. 19 while Fig. 20 presents the two hypothetical series.

As already mentioned, the C-value decreases with increasing diameter, due to the constant strength of the material. Therefore, in this representation, the abscissa values increase directly and the ordinates with the square of the enlargement factor.

In Fig. 20, a change in the circumferential speed of a decanter displaces the operating point with the slope 1. For scale-up from the pilot test, in which the point of critical throughput must be definitely identifiable, the possible limiting throughput for the intended machine is found and a decision is made whether this is adequate or an available machine with a larger capacity than required is selected.

It is recommended that the experiments be performed with the pilot decanter using the C-value of the designed large decanter, in order to exclude product effects dependent on acceleration.

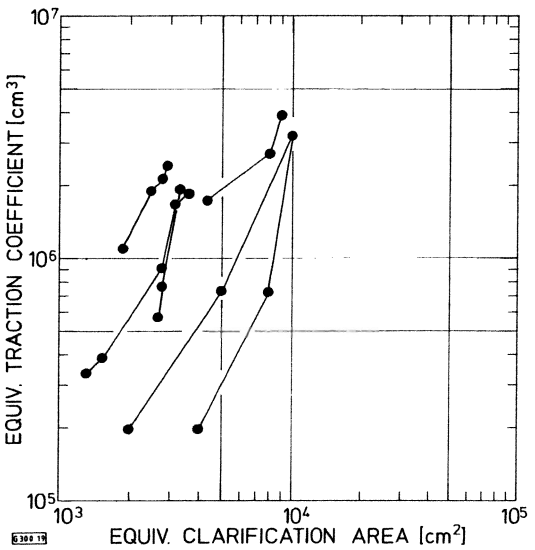

Fig. 19. Equivalent traction coefficient as a function of equivalent clarification area for different decanters.

Table 1. Two Hypothetical Construction Series.

type	diameter of cylinder [cm]	liquid height [cm]	thread height [cm]	number of thread	blade thickness [cm]	traction coefficient T [cm³]	clarification length L_{cyl} short [cm]	clarification length L_{cyl} long version [cm]	clarification area short [cm²]	clarification area long version [cm²]	C_{max} at $u = 80$ m/s	equiv. traction coefficient $S \times 10^6$ [cm³]	equiv. clarification area $\Sigma \times 10^6$ short [cm²]	equiv. clarification area $\Sigma \times 10^6$ long version [cm²]
A	25	3.75	6.25	2	0.37	77.3	37.5	50	2,945	3,927	5,220	0.404	15.374	20.499
B	32	4.8	8.0	2	0.48	162	48	64	4,825	6,434	4,175	0.67719	20.015	26.862
C	40	6.0	10	2	0.6	316	60	80	7,540	10,053	3,262	1.033	24.595	32.793
D	50	7.5	12.5	2	0.75	618	75	100	11,781	15,708	2,610	1.615	30.748	40.998
E	63	9.45	15.75	2	0.945	1,237	94.5	125	18,703	24,740	2,071	2.563	38.734	51.237
F	80	12.0	20	2	1.2	2,534	120	160	30,159	40,212	1,631	4.133	49.189	65.586
G	100	15.0	25	2	1.5	4,950	150	200	47,123	62,832	1,305	6.460	61.496	81.996
H	125	18.75	31.25	2	1.875	9,668	187.5	250	73,631	98,174	1,044	10.093	76.871	102.49
I	158	23.7	39.5	2	2.37	19,524	234	3,201	16,151	158,839	870	16.986	101.05	138.19

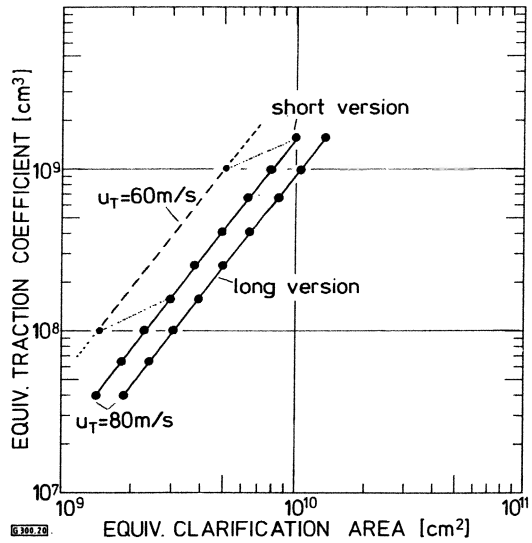

Fig. 20. Equivalent traction coefficient as a function of equivalent clarification area for hypothetical decanter series.

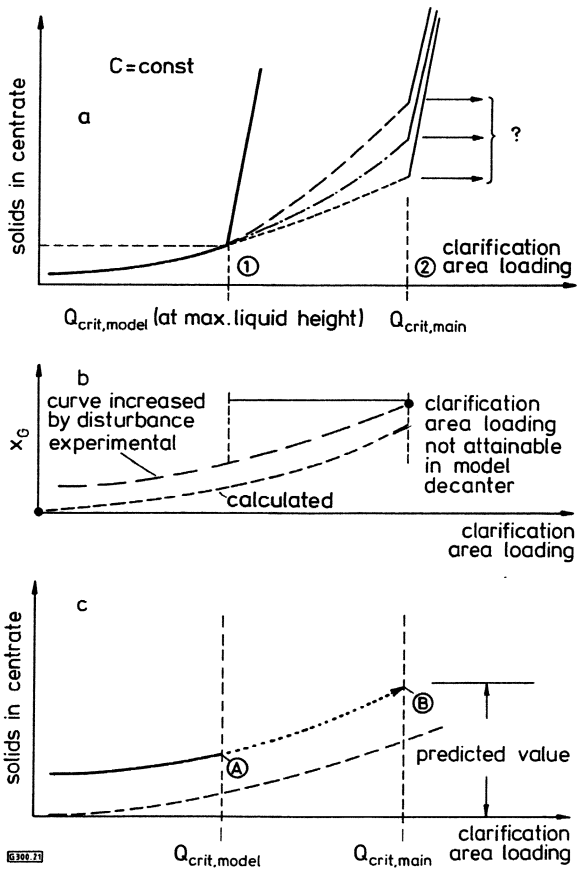

Fig. 21. Scale-up of pilot experiments.

This initially only provides the certainty that the clarification proceeds in the large machine without a disturbing drag effect; the solids content in the centrate cannot be, however, directly transferred from the operating range employed in the pilot machine.

At identical C-values, the machine ni larger has a critical throughput $(ni)^3$ times larger; the loading of the clarification area Q/A (at the same C-value) therefore reaches higher values in the large decanter.

This range of elevated clarification area loading, but not yet entering the drag effect range, cannot be operated in the model decanter; thus no indications can be obtained on an experimental basis regarding the further shape of the curve beyond point 1 (Fig. 21a).

For its determination not only by extrapolation, an estimation based on Stokes's law should be applied.

The limiting particle size is calculated as a function of the clarification loading and these pairs of values are plotted in Fig. 21b one above the other. In accordance with the method described in section 5, the solids in the centrate are calculated from the particle distribution curve.

The solids in centrate are also plotted against the clarification area loading (Fig. 21c). The curve is certainly lower than the measured one. However it can be determined purely by calculation up to the value $Q_{crit,main}/A$.

On the basis of this guideline, extrapolation of experimental values from A to B, still to be performed, now appears somewhat more realistic than without this theoretical aid (Fig. 21c).

From a certain amount of experience, it appears that the same disturbance effect of the screw motion can be achieved approximately at the same differential circumferential speed, and not at the same differential rotational speed between machines of different sizes.

For this reason it is recommended that the model tests should be conducted on the basis of a differential rotational speed higher by the enlargement factor subsequently selected.

In any case it must be ensured that the differential speed is sufficiently high for no build-up of solids to occur in the machine.

8. Influence of Drag Effect on Investment Costs of Clarification Decanters

The existing findings, i.e. that the clarification in decanting centrifuges is usually restricted by the drag effect, and now also the presented quantification, permit economic viability considerations of the investment costs. The prices of geometrically similar decanters but of different dimensions can be described approximately by the function

$$\log P = \log P_0 + m \log (d - d_0)$$

plotted in a log-log diagram (see Fig. 22). P_0 is the price of any given decanter with cylinder diameter d_0 from the given series. Gradients m will be different for the individual design series and they have no influence on the basic pattern of the following.

It is assumed that on process grounds (identical achievable residual moisture, identical specific flocculant requirement etc.) all decanters can be operated at identical centrifugal accelerations.

Table 2. Specific Costs of a Decanter Series.

Type		A	B	C	D	E	F	G	H	I
d_T		25	32	40	50	63	80	100	125	158
T		77.3	162.2	316.8	618.8	1,237.7	2,534	4,950	9,668	19,524
$\frac{T_i}{T_A}$		1	2.098	4.098	8.00	16.01	32.78	64.03	125.07	252.57
$p(m = 1.15)$		$1 = P_0$	1.972	2.532	2.60	2.817	3.001	3.156	3.3	3.42
$p(m = 1.3)$		$1 = P_0$	2.1	2.53	2.817	3.054	3.262	3.438	3.6	3.74
$p(m = 1.5)$		$1 = P_0$	2.26	2.764	3.097	3.37	3.61	3.812	4	4.165
$\frac{T_i}{T_A} : \frac{P_i}{P_0}$	at 1.15	1	1.064	1.742	3.077	5.683	10.92	20.28	37.9	73.85
	at 1.3	1	1.0	1.62	2.84	5.242	10.05	18.624	34.74	67.53
	at 1.5	1	0.928	1.483	2.58	4.751	9.08	16.8	31.26	66.71

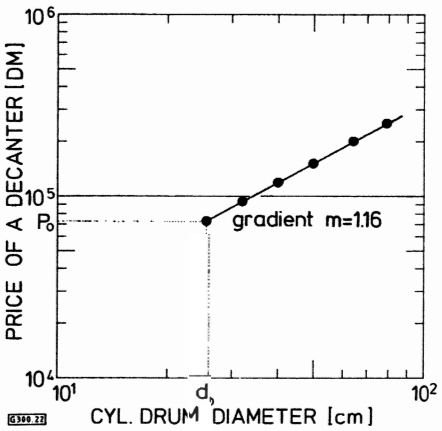

Fig. 22. The cost curve of a decanter series.

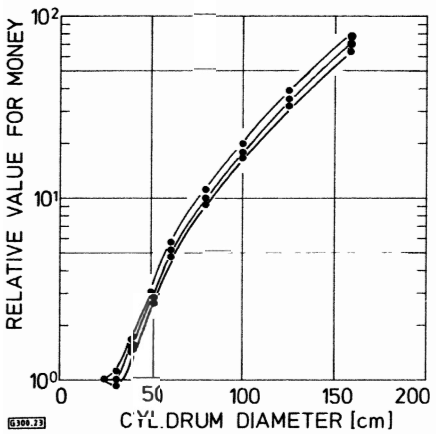

Fig. 23. Relative value for money of clarification decanters of different sizes.

If matching pairs of values of T and P are calculated, Table 2 results from an arbitrarily selected starting point of the smallest decanter (P_0 = standard value) of the hypothetical decanter series A to I and three freely chosen pitch values of $m = 1.15$; 1.3 and 1.5.

If the ratio of maximum throughput per price of any given machine to the maximum throughput per price of the small machine is determined and plotted against the drum radius, it can be seen that, in all the three different price progressions the characteristic parameter describing the "value for money" rises very steeply (Fig. 23).

It follows that, from the standpoint of investment costs, splitting of the production rate into two or more machines is uneconomical, and that the total capacity of one single large machine should always be used.

On the other hand, the theories considered here show that the possibilities of increasing the capacity by widening the screw pitch, increasing the liquid height and enlarging clarification area particularly apply to small and medium-sized machines.

9. Equipment Implications

9.1. Direct and Counterflow Decanter

The above mentioned laws apply initially only for the countercurrent decanter, in which the finer particles settle on a flat and very smooth bottom surface, abraded by the screw. The cocurrent decanter offers the superfine particles, subjected to drag force, a better protection against being flushed out. Most of the solids are transported from the feed zone at the end of the cylinder along its length and then form a cake which mainly covers the cylinder jacket. In this case, the superfine particles which are sedimented later find a less smooth, undulated cake surface. The undulations protect the solids from further flushing out. This process is probably the main reason for the high clarification efficiencies of cocurrent machines, compared to the countercurrent decanters, all other parameters remaining constant.

9.2. Increase of Liquid Height

Although Eq. (14) demonstrates that the critical throughput could be increased on a further increase of liquid height, the following limitations do arise:

- Mean acceleration value decreases with increasing liquid height; this reduces the efficiency of the centrifuge.
- Corresponding to a further increase in the liquid height, the cone would have to be lengthened in order to raise the level of the sludge. On account of problems connected with conveying of thin pasty sludges, the cone angle cannot, in general, be increased any further. This however leads to a longer, more expensive and dynamically less stable machine.
- Although tests up to values of $b_{Niv}/r_T = 0.31$ have shown a quadratic relationship, this range of very high liquid height settings is not yet sufficiently well known and it would be possible for the exponent on b_{Niv} to fall below 2. An increase in the level must therefore be viewed together with other processes and, in individual cases, carefully assessed.

9.3. Increase of Screw Pitch

An increase of the screw pitch is almost directly proportional to the throughput increase. However, auxiliary conditions must also be considered in relation to this change.

In the region of the cone, screw threads as flat and narrow as possible are required, particularly for conveying pasty sludges. An extension on the clarification side thus results in a conical transition zone of the screw channel, where the still high flow velocities prevailing in the feed zone (countercurrent decanter) are being continuously reduced. Transition of the screw pitch can only be achieved gradually, so as to avoid flow detachment at the channel walls [16].

9.4. Change of Flow Profile in Screw Channel

According to the equilibrium of forces, see Fig. 8, it is required to reduce the shear gradient at the bottom. This could be achieved by inserts, as shown in Fig. 24 [17].

9.5. Stopping of Dragged Particles

In a series of transverse grooves, impact or similar edges (Fig. 25), arranged near the end of the drum and drawn by

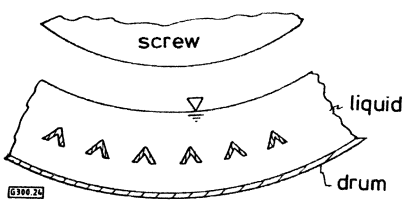

Fig. 24. Inserts in the screw channel.

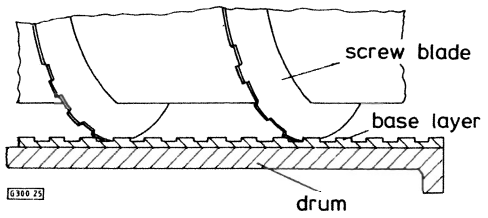

Fig. 25. Grooving in the base layer of a decanter.

the rotating screw in the base layer during each revolution, dragged particles could be held and nevertheless scraped together into a small cake in front of the conveyor blade. They could be conveyed to the solids discharge point without being again affected by the flow. Such configurations have already been tested in a channel in the gravity field, and a considerable increase was found in comparison to a smooth base.

9.6. Conveying of Centrate Outside the Screw Channels

In order to reduce flow velocities of the centrate in the rotor, some workers have already suggested that the liquid should flow along an axial path and not be forced into the screw channel. Resultant constructional solutions are ribbon screws, inserts with axial guide tubes and perforated screw blades. Although many such solutions have been known for a long time from the patent literature, the authors are not aware of any comparative tests having been performed. Neither have these solutions been widely adopted in practice.

10. Conclusions

In order to achieve reliable results, measurements must be taken in decanters of different sizes both on the laboratory and on industrial scale.

The authors intend to continue with this line of research over the next few years. It is hoped to receive practical support from and liase with industry. Cooperation of any interested person or organization will be appreciated.

Symbols used

A	[m^2]	clarification area
C	[−]	centrifugation value
D	[g/l]	solids in centrate
d_S	[m]	thickness of screw blade
d_T	[m]	rotor diameter
f	[−]	friction factor
F_A	[N]	pressing force
F_H	[N]	adhesive force
F_S	[N]	drag force
g	[m/s^2]	gravitational acceleration
b_{Niv}	[m]	liquid height
L_e	[m]	distance between inlet and overflow
n_H	[1/min]	absolute rotational speed
P	[DM]	price
P_0	[DM]	price standard value

Q_{susp}	[m^3/h]	suspension throughput
Q_{crit}	[m^3/h]	critical throughput
$Q_3(X)$	[m^3]	cumulative mass distribution
r_T	[m]	drum radius
S	[m^3]	equivalent traction coefficient
T	[m^3]	traction coefficient
v_m	[m/s]	mean velocity
w_{ST}	[m/s]	Stokes's settling velocity
x	[m]	particle diameter
x_G	[m]	limiting grain diameter
x_{min}	[m]	smallest particle diameter of particle distribution
x_s	[m]	drag particle diameter
z_s	[–]	number of screw threads
$\Delta\rho$	[kg/m^3]	difference between densities of solids and liquid
η	[Ns/m^2]	viscosity of liquid
ω	[rad/s]	angular velocity
α	[degree]	screw pitch angle

References

[1] Redeker, D., *Chem.-Ing.-Tech. 52* (1980) p. 542–543.
[2] Stahl, W., *Chem.-Ing.-Tech. 47* (1975) Nr. 20, p. 853.
[3] Smith, F. H., Hebb, M. H., in: *Encyclopedia of Chemical Technology* (Kirk, Otthmer), vol. 3, pp. 501–521, Interscience, New York 1949.
[4] Ambler, Ch. M., *Chem. Eng Prog. 48* (1952) Nr. 48, pp. 151–158.
[5] Ambler, Ch. M., *Ind. Eng Chem. 53* (1961) Nr. 6, pp. 430–433.
[6] Trawinski, H., in: *Encyklopädie der technischen Chemie* (Bartholomé, E., Biekert, E., Hellmann, H., Ley, H.), vol. 2, pp. 204–223, Verlag Chemie, Weinheim 1972.
[7] Gösele, W., *Habilitationsschrift,* Univ. Stuttgart 1971.
[8] Frampton, G. A., *Chem. Process Eng (London)* (1963) pp. 402–412.
[9] Müller, H.-W., Schaffer, J., Conrad, S., *Chem. Tech. (Leipzig) 32* (1980) Nr. 2, pp. 76–80.
[10] Alt, C., Faust, T., *Strömungs- und Absetzvorgänge in Vollmantel-Schneckenzentrifugen,* Arbeitsbericht über Al 93/15 und Al 93/18, Institut für Mechanische Verfahrenstechnik, Univ. Stuttgart 1981.
[11] Kannenberg, H.-H., *Diplomarbeit,* TH Braunschweig 1962.
[12] Anton, H., *Diplomarbeit,* TH Braunschweig 1962.
[13] Hesse, H., *Diplomarbeit,* TH Braunschweig 1962.
[14] Burger, M., *Diplomarbeit,* Univ. Karlsruhe 1980.
[15] Langeloh, T., *Diplomarbeit,* Univ. Karlsruhe 1981.
[16] P 3 139 345.4, Dekanter-Vorrichtung (Inv.: Stahl, W.).
[17] P 3 142 805.3, Dekantierzentrifuge (Inv.: Stahl, W.).

The Disposal of Exhaust Gases Containing Acetylene*

Peter Gentsch, Julius Jeisy and Wolfgang Bartknecht**

A process has been developed in which exhaust gases containing ethylene and acetylene can be burnt in the boiler house for steam generation, providing useful energy and with no danger to the environment. Since high concentrations of acetylene may occur and, even at low pressures, acetylene can decompose into carbon and hydrogen, special safety precautions must be taken. In order to prevent, in the event of ignition, the decomposition of acetylene with a consequent explosion or detonation in the exhaust gas line, the exhaust gas is mixed with natural gas in a jet-type mixer, immediately on leaving the production plant and fed to the burner. A flame arrester has been incorporated upstream of the burner to prevent flashback into the exhaust gas system. So far, methane/acetylene/air mixtures had not been used as test gases for flame arresters, and therefore a substitute test gas had to be found for which a test certificate was available. Experimental studies showed that a mixture of 80 vol.-% methane and 20 vol.-% acetylene has the same ignition properties and virtually the same explosion characteristics as propane.

1. Introduction

Large quantities of waste gases containing ethylene and acetylene pass through the exhaust system of a pharmaceutical plant. Acetylene, produced from calcium carbide, contains impurities comprising mainly traces of sulphur, hydrogen phosphide and ammonia, and constitutes a nuisance, on account of its penetrating smell. On economic grounds (calorific value H_u = 48,000 kJ/kg) an obvious solution is to burn the exhaust gas in a non-polluting manner for steam generation in the boiler house. This combustion can save considerable quantities of fuel and natural gas and at the same time reduce the environmental pollution to a minimum.

In crude oil distillation at atmospheric pressure, the light hydrocarbons are usually brought to heating gas pressure by means of rotary or piston type compressor systems and fed into the heating gas system [1]. Some control difficulties occur when mechanical compressors with widely varying input conditions are used. The required effort is rather high, not to mention the large investment costs of such a machine. In addition, another form of energy, e.g. electricity, must be

* Lecture at the Annual Meeting of Process Engineers, Basle 1982.

** Dipl.-Ing. P. Gentsch and Dipl.-Ing. J. Jeisy, F. Hoffmann-La Roche & Co. AG, TIng/Ch, CH-4002 Basle, Dr.-Ing. W. Bartknecht, Ciba-Geigy AG, Zentraler Sicherheitsdienst, CH-4002 Basle.

 0343-5539/84/0203-0084$02.50/0